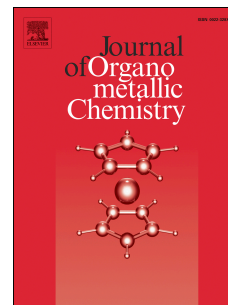


Accepted Manuscript

New highly cytotoxic organic and organometallic bexarotene derivatives

Yulia N. Nosova, Dmitry S. Karlov, Sergey A. Pisarev, Ilya A. Shutkov, Vladimir A. Palyulin, Mathurin Baquié, Elena R. Milaeva, Paul J. Dyson, Alexey A. Nazarov



PII: S0022-328X(17)30188-2

DOI: [10.1016/j.jorganchem.2017.03.031](https://doi.org/10.1016/j.jorganchem.2017.03.031)

Reference: JOM 19865

To appear in: *Journal of Organometallic Chemistry*

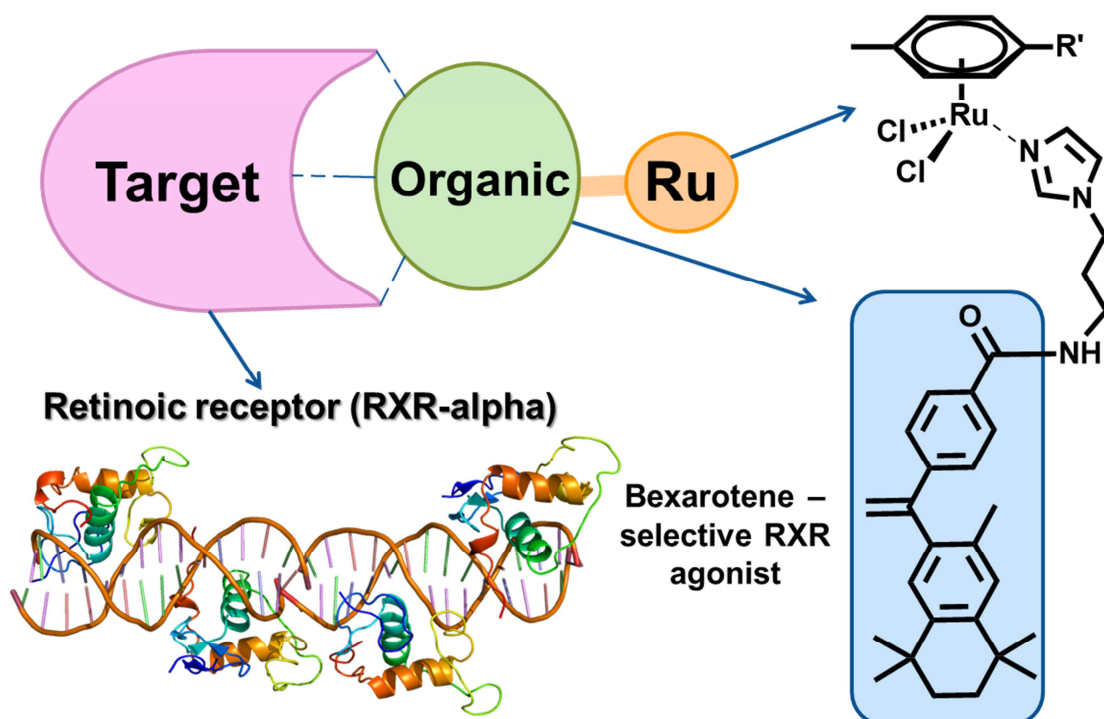
Received Date: 31 December 2016

Revised Date: 12 March 2017

Accepted Date: 15 March 2017

Please cite this article as: Y.N. Nosova, D.S. Karlov, S.A. Pisarev, I.A. Shutkov, V.A. Palyulin, M. Baquié, E.R. Milaeva, P.J. Dyson, A.A. Nazarov, New highly cytotoxic organic and organometallic bexarotene derivatives, *Journal of Organometallic Chemistry* (2017), doi: 10.1016/j.jorganchem.2017.03.031.

This is a PDF file of an unedited manuscript that has been accepted for publication. As a service to our customers we are providing this early version of the manuscript. The manuscript will undergo copyediting, typesetting, and review of the resulting proof before it is published in its final form. Please note that during the production process errors may be discovered which could affect the content, and all legal disclaimers that apply to the journal pertain.



Ruthenium(II) arene compounds modified with bexarotene, a retinoid that selectively activates retinoid X receptors, prepared by tethering bexarotene to the ruthenium fragment via an imidazole linker. Docking studies show that the interactions of these compounds with possible targets are significantly different to the binding mode of the parent drug.

New highly cytotoxic organic and organometallic bexarotene derivatives.

Yulia N. Nosova¹, Dmitry S. Karlov¹, Sergey A. Pisarev³, Ilya A. Shutkov¹, Vladimir A. Palyulin¹, Mathurin Baquie², Elena R. Milaeva¹, Paul J. Dyson², Alexey A. Nazarov¹

¹ *Lomonosov Moscow State University, Department of Medicinal Chemistry and Fine Organic Synthesis, Leninskie Gory 1/3, 119991 Moscow, Russian Federation*

² *Institute of Chemical Sciences and Engineering, Swiss Federal Institute of Technology Lausanne (EPFL), CH-1015 Lausanne, Switzerland.*

³ *Institute of Physiologically Active Compounds, Russian Academy of Science, Severny proezd, 142432, Chernogolovka, Moscow region, Russian Federation*

Abstract

A series of bifunctional ruthenium(II) arene compounds modified with bexarotene, a retinoid that selectively activates retinoid X receptors inducing cell differentiation and apoptosis and preventing drug resistance, are described. The bexarotene is tethered to the ruthenium(II) arene fragment via an imidazole linker. Both the bexarotene-imidazole ligand and ruthenium(II) arene complexes are considerably more cytotoxic than the parent drug bexarotene. Docking studies show that the interactions of these compounds with possible targets are significantly different to the binding mode of the parent drug.

Introduction

The discovery of the anticancer properties of cisplatin represents a significant breakthrough in the treatment several malignant tumors such as testicular and ovarian cancer [1]. Nowadays platinum-based compounds are involved in more than 50% of all anticancer chemotherapy regimens and are only limited by their strong side effects and incidents of drug resistance [2]. The clinical success of cisplatin initiated the search for other efficient metal-based anticancer agents and over the years large numbers of non-platinum metal-based compounds have been evaluated as antitumor agents [3, 4]. Ruthenium compounds are among the most promising

candidates with currently KP1339 and NAMI-A having entered clinical trials [5-7]. These ruthenium(III) compounds are considered to act as pro-drugs, possibly transforming into active Ru(II) species following reduction in the tumor environment [8].

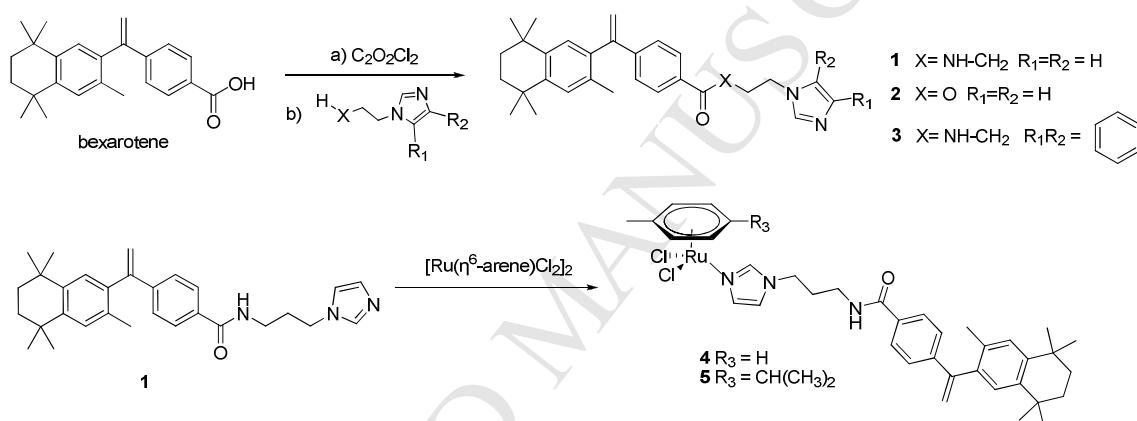
Another promising class of antitumor ruthenium-based compounds is based on the 'half-sandwich' Ru(II)-arene motif with RAPTA-C now in advanced pre-clinical studies [9, 10]. In comparison to platinum compounds, which preferentially bind to DNA [11, 12], RAPTA-C shows a strong preference for binding to proteins and, in particular, to histones [13, 14]. It has become evident that RAPTA-C is most effective when applied in combination with other drugs [15, 16], and an interesting strategy is to modify the RAPTA structure with a known drug, which operates via a complementary mechanism, to give a new bifunctional drug-like compound. Such an approach has been successfully achieved with various biologically active groups [17-19] attached via the η^6 -coordinated arene ligand [20-22] or by direct coordination to the metal center [23-29].

Bexarotene is a selective agonist of retinoid X receptors (RXRs), and is used to treat cutaneous T-cell lymphoma, inducing cell differentiation and apoptosis and inhibiting cancer metastasis [30-32]. Consequently, we decided to covalently link bexarotene to the Ru(II)-arene framework via an imidazole ligand since this approach has showed considerable potential with other classes of drugs [33-35]. In this paper, we describe the synthesis, characterization and biological evaluation of the new compounds.

Results and discussion

Synthesis of the imidazole ligands modified with bexarotene, **1-3**, was achieved *via* reaction of the acid-chloride of bexarotene (not isolated) and N-(aminopropyl)imidazole, 2-(1H-imidazol-1-yl)ethanol or 3-(1H-benzoimidazol-1-yl)propan-1-amine (Scheme 1). The cytotoxicity of bexarotene and **1-3** was evaluated against the ovarian cancer cell lines A2780 and A2780cisR, the former being sensitive to cisplatin and the latter having acquired resistance to cisplatin (Table 1). Compound **1** was found to be the most cytotoxic among all ligands; being ca. 500 fold more cytotoxic than the parent drug. In contrast, ligands **2** and **3** are only approximately twice as cytotoxic as bexarotene and therefore ruthenium derivatives and docking studies were performed using only ligand **1**. Subsequent reaction of **1** (i.e. the most cytotoxic ligand) with the dimers $[\text{Ru}(\eta^6\text{-arene})\text{Cl}_2]_2$ (arene = $\text{C}_6\text{H}_5\text{CH}_3$ toluene or $p\text{-C}_6\text{H}_4\text{CH}_2\text{CH}(\text{CH}_3)_2$ p-cymene), affords **4** and **5**. All organometallic compounds are soluble and stable in polar organic solvents such as CH_2Cl_2 and DMF. In DMSO/water (1% DMSO, since this is close to the concentration used in the cell

studies) **4** and **5** exist are present in an equilibrium between different forms, with the exchange of the Cl ligands by water being the major adduct, similar to that observed for RAPTA compounds. In addition, a minor component present in 1% DMSO in water involves substitution of the organic ligand, although full decomposition of the compounds was not observed [36]. All the compounds were characterized by ^1H and ^{13}C NMR spectroscopy, ESI mass spectrometry and elemental analysis. The ^1H and $^{13}\text{C}\{^1\text{H}\}$ NMR spectra confirm the expected structures of **1-5**. Coordination of ligand **1** to ruthenium centre leads to changes in the chemical shifts of the imidazole protons. The N-CH=CH protons are observed from 6.85 to 6.99 ppm, 7.58 to 7.89 and 7.09 to 7.16 for **1**, **4** and **5**, respectively. The dominant peak in the ESI mass spectra of ligands **1-3** correspond to the $[\text{M}+\text{H}]^+$ ion, whereas for complexes **4** and **5** the highest mass peak with the characteristic isotope pattern for ruthenium corresponds to the $[\text{M}-\text{Cl}]^+$ ion.



Scheme 1

The cytotoxicity of **4** and **5** on the same two cancer cell lines, i.e. A2780 and A2780cisR, is in the nanomolar range with the complexes being marginally less cytotoxic than **1**. To acquire more information on the selectivity **1**, **4** and **5**, which are all considerably more cytotoxic than bexarotene and cisplatin they were evaluated against immortalized non-tumorigenic human endothelial kidney (HEK) cells (Table 1). The three compounds display moderate cancer cell selectivity, being 2-3 fold less cytotoxic to the HEK cells relative to the ovarian cancer cell lines.

Table 1. Cytotoxicity of bexarotene, **1-5**, RAPTA-C, and cisplatin towards the ovarian cancer cell lines A2780 and A2780R and non-tumoural HEK cells.

Compound	IC ₅₀ μM		
	A2780	A2780R	HEK
1	0.027 ± 0.013	0.028 ± 0.017	0.065 ± 0.021
2	7.23 ± 0.38	8.51 ± 0.93	

3	9.82 ± 2.35	11.91 ± 2.40	
4	0.034 ± 0.004	0.028 ± 0.008	0.093 ± 0.033
5	0.075 ± 0.023	0.063 ± 0.034	0.147 ± 0.017
bexarotene	23.74 ± 1.38	27.37 ± 5.13	64.16 ± 18.09
RAPTA-C	>250	>250	
Cisplatin	9.5 ± 2.4	31.5 ± 3.4	

The dynamical behavior of RXR α adducts of **1** was evaluated over 35 ns using molecular dynamics simulations and compared to bexarotene. The hydrogen bonding analysis and ligand position in the RXR α ligand-binding domain were evaluated. While the bulky hydrophobic region of both compounds seems to have similar orientation and contacts, the hydrogen bonds between the receptor and compounds differs significantly. The carboxyl group of bexarotene forms a salt bridge with R316 maintaining hydrogen bonding network, with a sidechain Q275 and backbone atoms of A327, L309, and L325. The whole construction exists during almost all the simulation time and seems to be a very important feature for maintaining an active conformation of the receptor (Fig. 1). Compound **1** is unable to form a salt bridge with R316, which leads to an increase of the distance between loop 324-332 and helix 268 – 288 (Fig. 2), which may induce the transformation of the receptor to an inactive form [37].

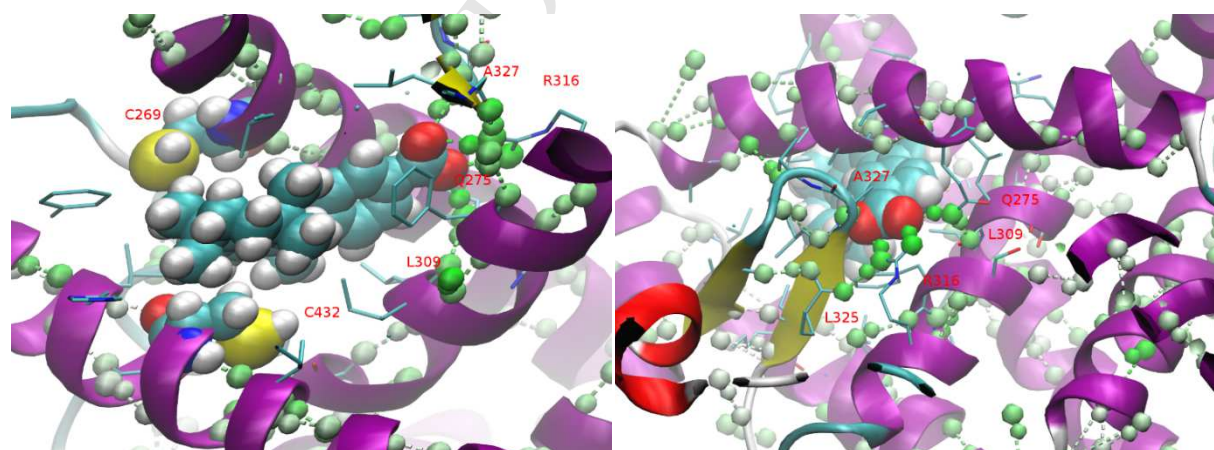


Fig. 1. Hydrogen bonding analysis of bexarotene - RXR α adducts from different views. The VdW spheres represent bexarotene and the green spheres represent hydrogen bonds. Color intensity is positively correlated with the lifetime of the considered bond during simulation.

At the same time, the imidazole fragment in **1** can take part in the hydrogen bonding networks with long lifetimes, which contain R371, E239 and S312. The binding energy contribution from residues 265 -275, 309-315 and 326-327 increase greatly for **1** in comparison to bexarotene. The hydrogen bond of the imidazole moiety with R371, which is absent in bexarotene, contributes to

the decreased binding energy of **1**, but cannot offset the losses in binding energy caused by a salt bridge disruption between the bexarotene carboxyl group and R316.

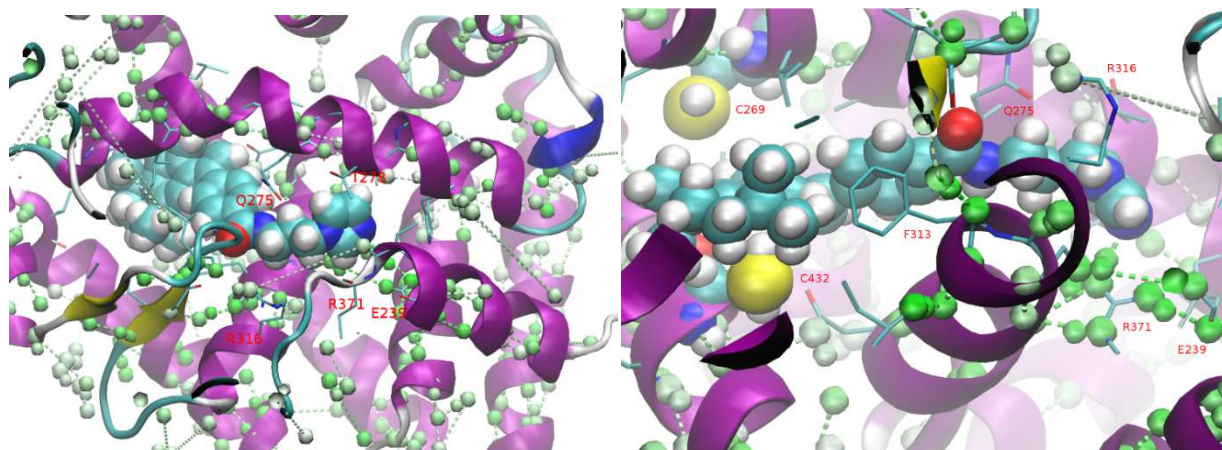


Fig. 2. Hydrogen bonding analysis of **1** - RXR α adducts from different views. The VdW spheres represent the **1** and the green spheres represent hydrogen bonds. The color intensity is positively correlated with the lifetime of considered bond during simulation.

A similar investigation was performed using compound **4**, it should be noted that **4** has internal degrees of freedom which cannot be assessed by molecular mechanics techniques accurately, due to internal rotation around the coordination bonds. Thus, a DFT-based relaxed potential energy scan was performed changing the dihedral angle as represented in Fig. 3. We observed three minima, which approximately match the scanned dihedral angle values of 90, 180 and 270°, and since the energy difference between them is relatively low (1-2 kcal/mol according to different methods) they were all used in the docking study. A relatively high energy was observed for **4** when the scanned dihedral angle was 0°, so it was not used for subsequent calculations due to a lower occupancy under physiological conditions.

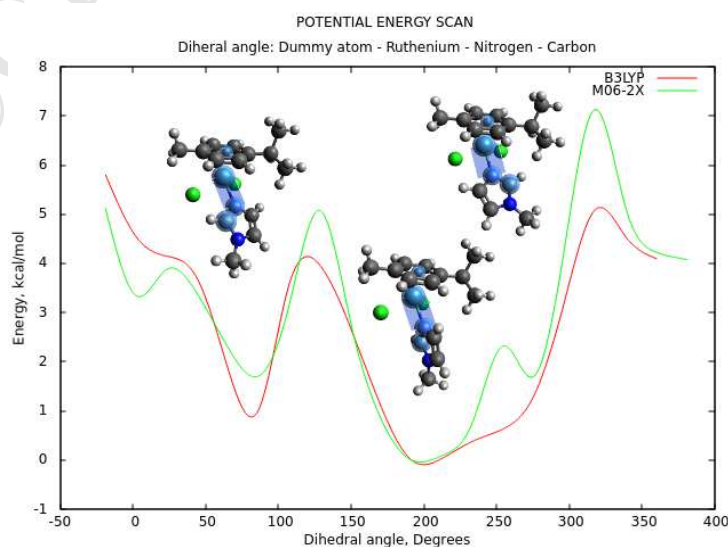


Fig. 3. Potential energy profile as a function of the dihedral angle in **4**. The red curve approximates the result of the B3LYP calculations and the green curve corresponds to the M06-2X calculations.

The optimum complex conformation obtained in the docking study is shown in Fig. 4. The position of the hydrophobic bexarotene moiety in the complex differs markedly from the position of this fragment in the adduct with bexarotene. The methylene fragment points in the opposite direction to that in bexarotene and it does not fill the entire space of the binding pocket. Interestingly, in comparison to the structure of **1**, the amide group maintains a hydrogen bond with the sidechain of Q275. In this case, the ruthenium ion lies at a distance of about 9 Å from the sulfur atom of M254. It is generally known that ruthenium forms stable complexes with sulfur containing compounds and although the distance is rather large, M254 is a part of a flexible loop (243 – 264), so the possibility of Ru – S bond formation is relatively high.

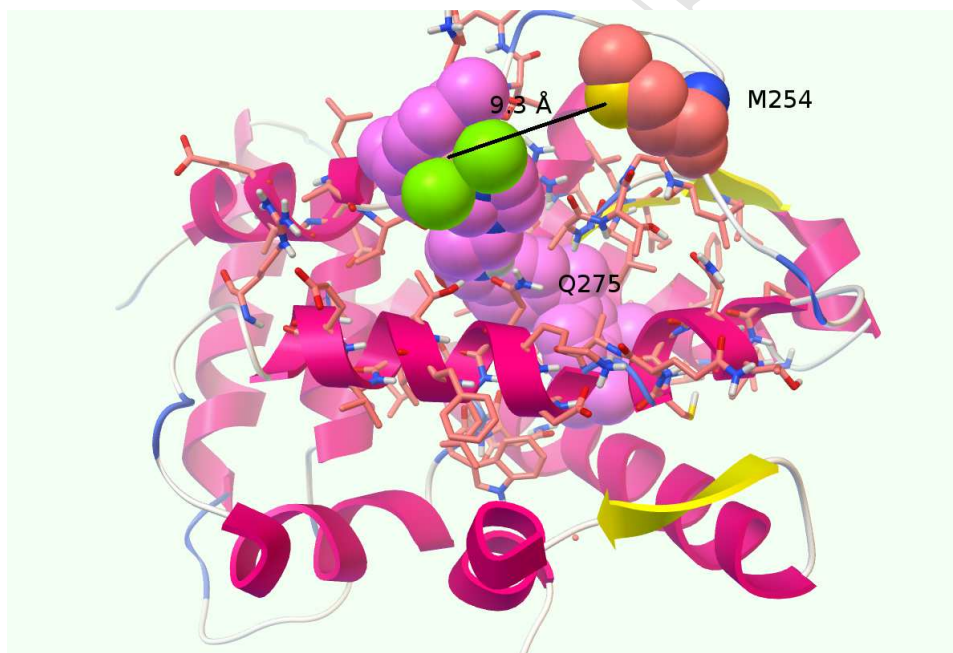


Fig. 4 Docking of **4** into RXR α binding domain. Spacefil representation was used for the ligand and M254 atoms.

Conclusions

Organometallic compounds in which bexarotene is tethered to the ruthenium(II) arene unit, i.e. complexes **4** and **5**, were prepared and found to exhibit a high cytotoxicity to human ovarian cancer cells, being more effective than cisplatin, and exhibiting a modest degree of cancer cell selectivity. In the process of preparing **4** and **5** it was found that the bexarotene-modified imidazole ligand **1**, which represents a novel bexarotene derivative, is two orders of magnitude more cytotoxic than bexarotene itself, while maintaining the same degree of cancer cell

selectivity. Therefore, in this case, the ligand exhibits more relevant anticancer properties than the organometallic derivatives, but it should be noted that **1** would not have been prepared without the view to using it as a ligand. Computer modelling was used to partly explain the molecular basis for the increased activity, with the imidazole group participating in H-bonding interaction with the RXR α receptor. But since the estimated binding free energy of **1** is significantly higher than the same value calculated for bexarotene complex the RXR α -receptor may not be the primary target for these modified bexarotene derivatives.

Experimental

Solvents were purified and degassed prior to use [38] ^1H and $^{13}\text{C}\{^1\text{H}\}$ NMR spectra were recorded on a Bruker Avance II 400 spectrometer at room temperature and were referenced to the residual ^1H signal of the NMR solvent. ESI-mass spectra of the compounds were obtained in MeOH on a ThermoFinnigan LCQ Deca XP Plus quadrupole ion-trap instrument operated in positive ion mode over a mass range of m/z 150-1000. The ionization energy was set at 3.5 kV and the capillary temperature at 150 °C. Melting points were determined with a Stuart Scientific SMP3 apparatus and are uncorrected. The Varian 971-FP flash chromatography system was used for compound purification. Elemental analyses were carried out by the microanalytical laboratory at the EPFL.

Synthesis of N-(3-(1H-imidazol-1-yl)propyl)-4-(1-(3,5,5,8,8-pentamethyl-5,6,7,8-tetrahydronaphthalen-2-yl)vinyl)benzamide, 1

An excess of oxalyl chloride (5 ml, 58.3 mmol) was added to a solution of 4-(1-(3,5,5,8,8-pentamethyl-5,6,7,8-tetrahydronaphthalen-2-yl)vinyl)benzoic acid (1.0 g, 2.87 mmol) in CH_2Cl_2 (50 mL). A catalytic amount of DMF (20 μl) was added and the reaction mixture was heated under reflux for 2 h. Unreacted oxalyl chloride and solvent were removed under reduced pressure to yield 4-(1-(3,5,5,8,8-pentamethyl-5,6,7,8-tetrahydronaphthalen-2-yl)vinyl)benzoyl chloride as a yellowish solid and was used without purification. N-(aminopropyl)imidazole (1.25 ml, 10.48 mmol) was added to a solution in CH_2Cl_2 (100 mL) and the reaction mixture was stirred for 6 h at the room temperature. Afterwards a solution of NaHCO_3 (5 %, 60 mL) was added to quench the reaction and the aqueous phase was extracted with CH_2Cl_2 (3 \times 50 mL). The organic fractions were combined and washed with brine (2 \times 50 mL), dried over Na_2SO_4 , and solvent was removed in vacuum. The pure product was obtained after column chromatography on silica gel with $\text{EtOH}/\text{CH}_2\text{Cl}_2$ 1:10 as eluent. Yield 1.04 g, (78.9%), elem. anal. calc (%) for ($\text{C}_{30}\text{H}_{37}\text{N}_3\text{O}$): C 79.08, H 8.19, N 9.22, found: C 78.87, H 8.37, N 9.17. ^1H NMR (400.13 MHz, CDCl_3) δ : 7.70 (d, 2H, $J = 8.5$ Hz, H_{Ar}), 7.58 (s, 1H, N- $\underline{\text{C}}\text{H}=\text{CH}$), 7.35 (d, 2H, $J = 8.5$ Hz, H_{Ar}), 7.14 (s, 1H, H_{Ar}), 7.09-7.07 (m, 2H, H_{Ar} , N- $\underline{\text{C}}\text{H}=\text{CH}$), 6.99 (s, 1H, N- $\underline{\text{C}}\text{H}=\text{N}$), 6.49 (t, 1H,

$J = 5.7$ Hz, NH), 5.80 (d, 1H, $J = 0.9$ Hz, C=CHH), 5.32 (d, 1H, $J = 0.9$ Hz, C=CHH), 4.08 (t, 2H, $J = 6.9$ Hz, NH-CH₂-CH₂-CH₂-N), 3.49 (q, 2H, $J = 6.5$ Hz, NH-CH₂-CH₂-CH₂-N), 2.11-2.18 (m, 2H, NH-CH₂-CH₂-CH₂-N), 1.95 (s, 3H; Ar-CH₃), 1.72 (s, 4H, C-CH₂-CH₂-C), 1.32 (s, 6H, C-(CH₃)₂), 1.29 (s, 6H, C-(CH₃)₂). ¹³C{¹H} (100.61 MHz, CDCl₃) δ : 167.7 (C=O), 149.1 (C=CH₂), 144.3 (C_{Ar}), 144.2 (C_{Ar}), 142.3 (C_{Ar}), 138.1 (C_{Ar}), 137.2 (CH_{Ar}), 133.0 (C_{Ar}), 132.7 (C_{Ar}), 129.7 (CH_{Ar}), 129.3 (CH_{Ar}), 128.0 (CH_{Ar}), 127.2 (CH_{Ar}), 126.7 (CH_{Ar}), 119.1 (CH_{Ar}), 116.4 (C=CH₂), 44.8 (N-CH₂), 37.2 (NH-CH₂), 35.2 (C-CH₂-CH₂-C), 34.0 (C-CH₂-CH₂-C), 33.9 (C-CH₂-CH₂-C), 32.0 (C-CH₃), 31.9 (C-CH₃), 31.1 (CH₂-CH₂-CH₂), 20.0 (Ar-CH₃). ESI-MS: m/z: 456 [M + H]⁺.

Synthesis of 2-(1H-imidazol-1-yl)ethyl 4-(1-(3,5,5,8,8-pentamethyl-5,6,7,8-tetrahydronaphthalen-2-yl)vinyl)benzoate 2

An excess of oxalyl chloride (5 ml, 58.3 mmol) was added to a solution of 4-(1-(3,5,5,8,8-pentamethyl-5,6,7,8-tetrahydronaphthalen-2-yl)vinyl)benzoic acid (1.0 g, 2.87 mmol) in CH₂Cl₂ (50 mL). A catalytic amount of DMF (20 μ l) was added and the reaction mixture was heated to reflux for 2 h. Unreacted oxalyl chloride and solvent were removed under reduced pressure to yield 4-(1-(3,5,5,8,8-pentamethyl-5,6,7,8-tetrahydronaphthalen-2-yl)vinyl)benzoyl chloride as a yellowish solid and was used without purification. 2-(1H-imidazol-1-yl)ethanol (1.1 g, 9.8 mmol) was added to a solution of the acid chloride in CH₂Cl₂ (100 mL) and the reaction mixture was stirred for 6 h at the room temperature, afterwards a solution of NaHCO₃ (5 %, 60 mL) was added to quench the reaction and the aqueous phase was extracted with CH₂Cl₂ (3 \times 50 mL). The organic fractions were combined and washed with brine (2 \times 50 mL), dried over Na₂SO₄, and solvent was removed in vacuum. The pure product was obtained after column chromatography on silica gel with EtOH/CH₂Cl₂ 1:10 as eluent. Yield 1 g, (78.7%), elem. anal. calc (%) for (C₂₉H₃₄N₂O₂): C 78.70, H 7.74, N 6.33, found: C 78.89, H 8.03, N 6.40. ¹H NMR (400.13 MHz, CDCl₃) δ : 7.97-7.91 (m, 2H, H_{Ar}), 7.59 (s, 1H, N-CH=CH), 7.35-7.38 (m, 2H, H_{Ar}), 7.14 (s, 1H, H_{Ar}), 7.11-7.10 (m, 2H, H_{Ar}, N-CH=CH), 7.03 (t, 1H, $J = 1.2$ Hz, N-CH=N), 5.84 (d, 1H, $J = 1.3$ Hz, C=CHH), 5.36 (d, 1H, $J = 1.2$ Hz, C=CHH), 4.59 (t, 2H, $J = 5.3$ Hz, O-CH₂-CH₂-N), 4.35 (t, 2H, $J = 5.3$ Hz, O-CH₂-CH₂-N), 1.95 (s, 3H; Ar-CH₃), 1.72 (s, 4H, C-CH₂-CH₂-C), 1.33 (s, 6H, C-(CH₃)₂), 1.30 (s, 6H, C-(CH₃)₂). ¹³C{¹H} (100.61 MHz, CDCl₃) δ : 165.8 (C=O), 149.0 (C=CH₂), 146.1 (C_{Ar}), 144.4 (C_{Ar}), 142.4 (C_{Ar}), 137.9 (C_{Ar}), 137.5 (CH_{Ar}), 132.7 (C_{Ar}), 129.9 (CH_{Ar}), 129.7 (CH_{Ar}), 128.1 (CH_{Ar}), 128.1 (C_{Ar}), 128.0 (CH_{Ar}), 126.8 (CH_{Ar}), 119.1 (CH_{Ar}), 117.1 (C=CH₂), 63.7 (O-CH₂), 45.9 (N-CH₂), 35.2 (C-CH₂-CH₂-C), 34.0 (C-CH₂-CH₂-C), 33.9 (C-CH₂-CH₂-C), 32.0 (C-CH₃), 31.9 (C-CH₃), 20.0 (Ar-CH₃). ESI-MS: m/z: 443 [M + H]⁺.

Synthesis of N-(3-(1H-benzo[d]imidazol-1-yl)propyl)-4-(1-(3,5,5,8,8-pentamethyl-5,6,7,8-tetrahydronaphthalen-2-yl)vinyl)benzamide 3

An excess of oxalyl chloride (5 ml, 58.3 mmol) was added to a solution of 4-(1-(3,5,5,8,8-pentamethyl-5,6,7,8-tetrahydronaphthalen-2-yl)vinyl)benzoic acid (1.0 g, 2.87 mmol) in CH₂Cl₂ (50 mL). A catalytic amount of DMF (20 μl) was added and the reaction mixture was heated to reflux for 2 h. Unreacted oxalyl chloride and solvent were removed under reduced pressure to yield 4-(1-(3,5,5,8,8-pentamethyl-5,6,7,8-tetrahydronaphthalen-2-yl)vinyl)benzoyl chloride as a yellowish solid and was used without purification. 3-(1H-benzo[d]imidazol-1-yl)propan-1-amine (1.5 g, 8.6 mmol) was added to a solution of the acid chloride in CH₂Cl₂ (100 mL) and the reaction mixture was stirred for 6 h at the room temperature, afterwards a solution of NaHCO₃ (5 %, 60 mL) was added to quench the reaction and the aqueous phase was extracted with CH₂Cl₂ (3 × 50 mL). The organic fractions were combined and washed with brine (2 × 50 mL), dried over Na₂SO₄, and solvent was removed under vacuum. The pure product was obtained after column chromatography on silica gel with EtOH/CH₂Cl₂ 1:10 as eluent. Yield 0.9 g, (62.0%), elem. anal. calc (%) for (C₃₄H₃₉N₃O): C 80.75, H 7.77, N 8.31, found: C 80.57, H 7.87, N 8.45. ¹H NMR (400.13 MHz, CDCl₃) δ: 8.01 (s, 1H, N-CH=N), 7.84-7.82 (m, 1H, H_{Ar}), 7.62 (d, 2H, *J* = 8.3 Hz, H_{Ar}), 7.45-7.42 (m, 1H, H_{Ar}), 7.35 (d, 2H, *J* = 8.4 Hz, H_{Ar}), 7.32-7.30 (m, 2H, H_{Ar}), 7.14 (s, 1H, H_{Ar}), 7.10 (s, 1H, H_{Ar}), 6.17 (s, 1H, NH), 5.81 (d, 1H, *J* = 1.2 Hz, C=CHH), 5.33 (d, 1H, *J* = 1.1 Hz, C=CHH), 4.33 (t, 2H, *J* = 6.9 Hz, NH-CH₂-CH₂-CH₂-N), 3.53 (q, 2H, *J* = 6.6 Hz, NH-CH₂-CH₂-CH₂-N), 2.26 (p, 2H, NH-CH₂-CH₂-CH₂-N), 1.96 (s, 3H; Ar-CH₃), 1.72 (s, 4H, C-CH₂-CH₂-C), 1.33 (s, 6H, C-(CH₃)₂), 1.30 (s, 6H, C-(CH₃)₂). ¹³C{¹H} (100.61 MHz, CDCl₃) δ: 167.7 (C=O), 149.0 (C=CH₂), 144.4 (C_{Ar}), 144.4 (C_{Ar}), 143.9 (C_{Ar}), 143.0 (CH_{Ar}), 142.3 (C_{Ar}), 138.0 (C_{Ar}), 133.6 (C_{Ar}), 132.8 (C_{Ar}), 132.7 (C_{Ar}), 128.0 (CH_{Ar}), 126.9 (CH_{Ar}), 126.8 (CH_{Ar}), 123.1 (CH_{Ar}), 122.3 (CH_{Ar}), 120.5 (CH_{Ar}), 116.5 (C=C_{CH}), 109.58 (CH_{Ar}), 42.9 (N-CH₂), 37.5 (NH-CH₂), 35.2 (C-CH₂-CH₂-C), 34.0 (C-CH₂-CH₂-C), 33.9 (C-CH₂-CH₂-C), 32.0 (C-CH₃), 31.9 (C-CH₃), 30.0 (CH₂-CH₂-CH₂), 19.9 (Ar-CH₃). ESI-MS: m/z: 506 [M + H]⁺.

Synthesis of dichlorido(η⁶-toluene)(N-(3-(1H-imidazol-1-yl)propyl)-4-(1-(3,5,5,8,8-pentamethyl-5,6,7,8 tetrahydronaphthalen-2-yl)vinyl)benzamide) ruthenium(II), 4

Solution of [(η⁶-toluene)RuCl(μ-Cl)]₂ (211.0 mg, 0.4 mmol) in CH₂Cl₂ (10 mL) was added to a solution of N-(3-(1H-imidazol-1-yl)propyl)-4-(1-(3,5,5,8,8-pentamethyl-5,6,7,8 tetrahydronaphthalen-2-yl)vinyl)benzamide (**1**) (377.0 mg, 0.83 mmol) in CH₂Cl₂ (30 mL) and the mixture was stirred at room temperature for 12 h. The reaction mixture was concentrated to

~5 mL and pentane (150 mL) was added to precipitate the product, the orange solid was washed with pentane (3 × 10 mL) and dried in vacuum. Yield 374.0 mg, (62.6 %), m.p. 163-164 °C (decomp.), elem. anal. calc (%) for C₃₇H₄₅Cl₂N₃ORu: C 61.74, H 6.30, N 5.83, found: C 61.98, H 6.55, N 5.67, ¹H NMR (400.13 MHz, CDCl₃) δ: 7.89 (s, 1H, N-CH=CH), 7.81 (d, 2H, J = 8.5 Hz, H_{Ar}), 7.34 (d, 2H, J = 8.5 Hz, H_{Ar}), 7.18 (s, 1H, H_{Ar}), 7.13 (s, 1H, N-CH=CH), 7.07 (s, 1H, H_{Ar}), 6.90 (brs, 1H, NH), 6.86 (s, 1H, N-CH=N), 5.79 (d, 1H, J = 1.2 Hz, C=CHH), 5.60 (t, 2H, J = 5.6 Hz, CH_{toluene}), 5.48 (t, 1H, J = 5.3 Hz, CH_{toluene}), 5.29 (s, 2H, CH_{toluene}), 5.28 (s, 1H; C=CHH), 3.79 (t, 2H, J = 6.4 Hz, NH-CH₂-CH₂-CH₂-N), 3.29 (q, 2H, J = 4.4 Hz, NH-CH₂-CH₂-CH₂-N), 2.17 (s, 3H; CH₃), 1.95 (s, 3H, CH₃), 1.85 (m, 2H, NH-CH₂-CH₂-CH₂-N), 1.69 (s, 4H; C-CH₂-CH₂-C), 1.29 (s, 6H; C-(CH₃)₂), 1.27 (s, 6H; C-(CH₃)₂), ¹³C{¹H} (100.61 MHz, CDCl₃) δ: 167.5 (C=O), 149.2 (C=CH₂), 144.3 (C_{Ar}), 144.0 (C_{Ar}), 142.3 (C_{Ar}), 140.5 (CH_{Ar}), 138.3 (C_{Ar}), 132.9 (C_{Ar}), 132.8 (C_{Ar}), 131.9 (C_{Ar}), 130.5 (C_{Ar}), 128.0 (CH_{Ar}), 127.7 (CH_{Ar}), 126.6 (CH_{Ar}), 119.9 (N-CH=N), 116.2 (C=CH₂), 99.6 (C_{toluene}), 86.3 (C_{toluene}), 81.1 (C_{toluene}), 79.5 (C_{toluene}), 46.0 (N-CH₂), 36.7 (NH-CH₂), 35.2 (C-CH₂-CH₂-C), 34.0 (C-CH₂-CH₂-C), 33.9 (C-CH₂-CH₂-C), 32.0 (C-CH₃), 31.9 (C-CH₃), 30.5 (CH₂-CH₂-CH₂), 20.0 (CH₃), 19.0 (CH₃), ESI-MS: m/z: 684 [M - Cl]⁺.

Synthesis of dichlorido(η⁶-p-cymene)(N-(3-(1H-imidazol-1-yl)propyl)-4-(1-(3,5,5,8,8-pentamethyl-5,6,7,8 tetrahydronaphthalen-2-yl)vinyl)benzamide) ruthenium(II), 5

To a solution of N-(3-(1H-imidazol-1-yl)propyl)-4-(1-(3,5,5,8,8-pentamethyl-5,6,7,8 tetrahydronaphthalen-2-yl)vinyl)benzamide (**1**) (500 mg, 1.1 mmol) in CH₂Cl₂ (30 mL), [(η⁶-p-cymene)RuCl(μ-Cl)]₂ (320 mg, 0.52 mmol) was added and the mixture was stirred at room temperature for 12 h. The reaction mixture was concentrated to ~10 mL and pentane (150 mL) was added to precipitate the product. The orange solid was washed with pentane and dried in vacuum. Yield 384 mg, (45.8%), m.p. 177-178 °C decomp., elem. anal. calc (%) for C₄₀H₅₁Cl₂N₃ORu: C 63.06, H 6.75, N 5.52, found: C 63.22, H 6.77, N 5.39, ¹H NMR (400.13 MHz, CDCl₃) δ 7.90 (d, 2H, J = 5.1 Hz, H_{Ar}), 7.87 (s, 1H, N-CH=CH), 7.36 (d, 2H, J = 7.9 Hz, H_{Ar}), 7.16 (s, 2H, N-CH=CH, H_{Ar}), 6.85 (s, 1H, N-CH=N), 5.81 (s, 1H, C=CHH), 5.44 (d, 2H, J = 5.7 Hz, CH_{p-cymene}), 5.31 (s, 1H; C=CHH), 5.23 (d, 2H, J = 5.7 Hz, CH_{p-cymene}), 3.73 (s, 2H, NH-CH₂-CH₂-CH₂-N), 3.28 (s, 2H; NH-CH₂-CH₂-CH₂-N), 2.88-2.99 (m, 1H, CH(CH₃)₂), 2.10 (s, 3H; CH₃), 1.97 (s, 3H; CH₃), 1.72 (s, 6H; C-CH₂-CH₂-C, NH-CH₂-CH₂-CH₂-N), 1.27-1.32 (m, 18H; C-(CH₃)₂, C-(CH₃)₂, CH(CH₃)₂). ¹³C{¹H} (100.61 MHz, CDCl₃) δ 167.4 (C=O), 149.3 (C=CH₂), 144.2 (C_{Ar}), 143.9 (C_{Ar}), 142.2 (C_{Ar}), 140.2 (CH_{Ar}), 138.3 (C_{Ar}), 132.9 (CH_{Ar}), 132.8 (CH_{Ar}), 131.5 (C_{Ar}), 129.3 (C_{Ar}), 128.0 (CH_{Ar}), 127.7 (CH_{Ar}), 126.5 (CH_{Ar}), 119.8 (CH_{Ar}), 116.2 (C=CH₂), 102.7 (C_{p-cymene}), 97.2 (C_{p-cymene}), 82.7 (CH_{p-cymene}), 81.3 (CH_{p-cymene}), 45.7 (N-CH₂), 36.5 (NH-CH₂), 35.2 (C-CH₂-CH₂-C), 34.0 (C-CH₂-CH₂-C), 33.9 (C-CH₂-CH₂-C), 32.0 (C-

$\underline{\text{C}}\text{H}_3$), 31.9 ($\text{C}-\underline{\text{C}}\text{H}_3$), 30.7 ($\text{CH}_2-\underline{\text{C}}\text{H}_2-\text{CH}_2$), 30.5 ($\underline{\text{C}}\text{H}(\text{CH}_3)_2$), 22.3 ($\text{CH}(\underline{\text{C}}\text{H}_3)_2$), 20.0 ($\underline{\text{C}}\text{H}_3$), 18.4 ($\underline{\text{C}}\text{H}_3$), ESIMS: m/z : 726 $[\text{M} - \text{Cl}]^+$.

Quantum Chemical Calculations

Calculations were performed using the version 3.0.2 of the ORCA quantum chemistry package[39]. We used the popular hybrid density functional B3LYP[40, 41] (in the formulation developed from the Ansatz V[42]) along with more recent M062X of the so-called 'Minnesota family' [43] with the M06L local part [44] and increased amount of the nonlocal Hartree-Fock exchange included in density functional theory (DFT) calculations. The value of the HF / total exchange fraction in M062X is doubled to 54% against the original 27% in M06[44] (it is only 20% in B3LYP). Los Alamos (LANL) effective core potential (ECP) with the corresponding basis sets was used for ruthenium ion [45].

Molecular dynamics simulations

The 3D structure of RXR α complex was taken from Protein Data Bank (PDB ID: 1MVC)[46]. All molecular dynamics (MD) simulations were performed using Amber 11 package[47]. Force field parameters set for protein and ligands atoms were derived from FF10 and GAFF [48]. Bexarotene was used in the deprotonated state; values of charges on ligands atoms were calculated using the semi-empirical AM1BCC method [49]. Two systems were simulated: the bexarotene bound form of RXR α ligand binding domain and **1**-bound form (this complex structure was obtained using the docking protocol, described below). All structures were solvated, placed into a truncated octahedron and then surrounded by a 10 Å water layer. Sodium ions were added to achieve charge neutrality of protein (12 Asp, 19 Glu, 12 Arg and 13 Lys residues). The simulation protocol included the following steps: (1) 500 steepest descent minimization steps and 500 conjugate gradient steps were applied to each system; (2) 50 ps of constant volume simulation were performed to increase temperature to 300 K; (3) 50 ps of constant pressure simulation were performed in order to drive the system density to the equilibrium state. Harmonic restraints were applied to protein and ligand atoms with 10 kcal/mol value during the last two stages; (4) after removal of the restraints, a 35 ns MD simulation was performed. Data for hydrogen bond [50] and MMPBSA [51] analysis were collected for the last 25 ns. The constant temperature was maintained using the Langevin thermostat. The integration step value of 2 fs was chosen in combination with SHAKE algorithm. Visualization and appropriate analysis were performed by VMD [52]. Graphs were created using the efficient scripting tool Gnuplot .

Docking studies

The docking study was carried out using AUTODOCK 4.2 [53] and the results were visualized with MGL Tools 1.5.6. Each docking calculation consisted of 200 launches of Lamarckian genetic algorithm. Since the ruthenium parameters are not available in the Autodock default parameter set, the vdW radius, the vdW well depth, the atomic solvation volume and the atomic solvation parameter were derived as follows. First two parameters were taken from the Rappe work [54]. Atomic solvation volume can be easily obtained using the simple formula: $\frac{4}{3} * \pi * (R_{vdw})^3$. Atomic solvation parameter adopts the same value among all default transition metals, so we decided to use it in this case. Protein sidechains were not allowed to be flexible. Bonds in the internal sphere of the structures were frozen to prevent conformational change in optimized structures.

Cell culture and inhibition of cell growth

Human A2780 and A2780cisR ovarian carcinoma cells were obtained from the European Centre of Cell Cultures (ECACC, Salisbury, UK) and maintained in culture as described by the provider. The cells were grown in Dulbecco's Modified Eagle Medium (DMEM) medium containing 4.5 g/L glucose, 5% heat-inactivated fetal calf serum (FCS) and penicillin/streptomycin (all cell culture reagents were obtained from Invitrogen, Basel, Switzerland). Unless otherwise specified, cells were grown for 24 h in 96-well plates (Costar, Corning, NY, USA), then the compounds (stock solution in DMSO) were added for the indicated times and concentrations. DMSO final concentration never exceeded 1%; at concentrations below 1% DMSO has no effect on cell survival (results not shown). Following exposure to the compounds, cell viability was assessed using the MTT assay (3-(4,5-dimethyl-2-thiazoyl)-2,5-diphenyltetrazolium bromide, Sigma-Aldrich, 200 µg/ml final concentration. Absorbance at 540 nm was measured in a multi-well plate reader (iEMS Reader, Labsystems, Bioconcept, Allschwil, Switzerland) and the absorbance values of treated cells were compared to the absorbance values of untreated cells. Experiments were conducted in duplicate wells and repeated at least twice.

Acknowledgements

We thank the Russian Science Foundation grant No. 14-03-00483 for financial support.

References

- [1] B. Rosenberg, L. Vancamp, T. Krigas, *Nature*, 205 (1965) 698-699.
- [2] M.A. Fuertes, C. Alonso, J.M. Pérez, *Chem. Rev.*, 103 (2003) 645-662.
- [3] Z. Guo, P.J. Sadler, *Angew. Chem., Int. Ed. Engl.*, 38 (1999) 1512-1531.

- [4] Y.N. Nosova, L.S. Foteeva, I.V. Zenin, T.I. Fetisov, K.I. Kirsanov, M.G. Yakubovskaya, T.A. Antonenko, V.A. Tafeenko, L.A. Aslanov, A.A. Lobas, M.V. Gorshkov, M. Galanski, B.K. Keppler, A.R. Timerbaev, E.R. Milaeva, A.A. Nazarov, *Eur. J. Inorg. Chem.*, (2016) in press.
- [5] M.A. Jakupec, M. Galanski, V.B. Arion, C.G. Hartinger, B.K. Keppler, *Dalton Transactions*, (2008) 183-194.
- [6] R. Trondl, P. Heffeter, C.R. Kowol, M.A. Jakupec, W. Berger, B.K. Keppler, *Chem. Sci.*, 5 (2014) 2925-2932.
- [7] A. Bergamo, T. Riedel, P.J. Dyson, G. Sava, *Invest. New Drugs*, 33 (2015) 53-63.
- [8] E. Alessio, *Eur. J. Inorg. Chem.*, (2016) n/a-n/a.
- [9] A. Weiss, R.H. Berndsen, M. Dubois, C. Muller, R. Schibli, A.W. Griffioen, P.J. Dyson, P. Nowak-Sliwinska, *Chem. Sci.*, 5 (2014) 4742-4748.
- [10] B.S. Murray, M.V. Babak, C.G. Hartinger, P.J. Dyson, *Coord. Chem. Rev.*, 306, Part 1 (2016) 86-114.
- [11] M. Galanski, V.B. Arion, M.A. Jakupec, B.K. Keppler, *Curr Pharm Des*, 9 (2003) 2078-2089.
- [12] B. Wu, G.E. Davey, A.A. Nazarov, P.J. Dyson, C.A. Davey, *Nucleic Acids Res.*, 39 (2011) 8200-8212.
- [13] B. Wu, M.S. Ong, M. Groessl, Z. Adhireksan, C.G. Hartinger, P.J. Dyson, C.A. Davey, *Chemistry – A European Journal*, 17 (2011) 3562-3566.
- [14] Z. Adhireksan, G.E. Davey, P. Campomanes, M. Groessl, C.M. Clavel, H. Yu, A.A. Nazarov, C.H.F. Yeo, W.H. Ang, P. Dröge, U. Rothlisberger, P.J. Dyson, C.A. Davey, *Nat Commun*, 5 (2014).
- [15] A. Weiss, X. Ding, J.R. van Beijnum, I. Wong, T.J. Wong, R.H. Berndsen, O. Dormond, M. Dallinga, L. Shen, R.O. Schlingemann, R. Pili, C.-M. Ho, P.J. Dyson, H. van den Bergh, A.W. Griffioen, P. Nowak-Sliwinska, *Angiogenesis*, 18 (2015) 233-244.
- [16] A. Weiss, D. Bonvin, R.H. Berndsen, E. Scherrer, T.J. Wong, P.J. Dyson, A.W. Griffioen, P. Nowak-Sliwinska, *Sci. Rep.*, 5 (2015) 8990.
- [17] V.B. Arion, A. Dobrov, S. Goschl, M.A. Jakupec, B.K. Keppler, P. Rapta, *Chem. Commun.*, 48 (2012) 8559-8561.
- [18] W. Kandioller, E. Balsano, S.M. Meier, U. Jungwirth, S. Goschl, A. Roller, M.A. Jakupec, W. Berger, B.K. Keppler, C.G. Hartinger, *Chem. Commun.*, 49 (2013) 3348-3350.
- [19] I. Turel, J. Kljun, F. Perdih, E. Morozova, V. Bakulev, N. Kasyanenko, J.A.W. Byl, N. Osheroff, *Inorg. Chem.*, 49 (2010) 10750-10752.
- [20] W.H. Ang, L.J. Parker, A. De Luca, L. Juillerat-Jeanneret, C.J. Morton, M. Lo Bello, M.W. Parker, P.J. Dyson, *Angew Chem Int Ed Engl*, 48 (2009) 3854-3857.
- [21] A.A. Nazarov, S.M. Meier, O. Zava, Y.N. Nosova, E.R. Milaeva, C.G. Hartinger, P.J. Dyson, *Dalton Trans*, 44 (2015) 3614-3623.
- [22] A.A. Nazarov, J. Risse, W.H. Ang, F. Schmitt, O. Zava, A. Ruggi, M. Groessl, R. Scopelitti, L. Juillerat-Jeanneret, C.G. Hartinger, P.J. Dyson, *Inorg. Chem.*, 51 (2012) 3633-3639.
- [23] M. Benadiba, M.C.I. de, R.L. Santos, F.O. Serachi, D. de Oliveira Silva, A. Colquhoun, *J. Biol. Inorg. Chem.*, 19 (2014) 1025-1035.
- [24] R. Pettinari, F. Marchetti, F. Condello, C. Pettinari, G. Lupidi, R. Scopelliti, S. Mukhopadhyay, T. Riedel, P.J. Dyson, *Organometallics*, 33 (2014) 3709-3715.
- [25] J.C.S. Lopes, J.L. Damasceno, P.F. Oliveira, A.P.M. Guedes, D.C. Tavares, V.M. Deflon, N.P. Lopes, M. Pivatto, A.A. Batista, P.I.S. Maia, G. Von Poelhsitz, *J. Braz. Chem. Soc.*, 26 (2015) 1838-1847.
- [26] G. Agonigi, T. Riedel, S. Zacchini, E. Păunescu, G. Pampaloni, N. Bartalucci, P.J. Dyson, F. Marchetti, *Inorg. Chem.*, 54 (2015) 6504-6512.
- [27] C.M. Clavel, P. Nowak-Sliwinska, E. Paunescu, A.W. Griffioen, P.J. Dyson, *Chem. Sci.*, 6 (2015) 2795-2801.
- [28] P. Nowak-Sliwinska, C.M. Clavel, E. Păunescu, M.T. te Winkel, A.W. Griffioen, P.J. Dyson, *Mol. Pharmaceutics*, 12 (2015) 3089-3096.

- [29] E. Păunescu, S. McArthur, M. Soudani, R. Scopelliti, P.J. Dyson, *Inorg. Chem.*, 55 (2016) 1788-1808.
- [30] W.C. Yen, R.Y. Prudente, M.R. Corpuz, A. Negro-Vilar, W.W. Lamph, *Br J Cancer*, 94 (2006) 654-660.
- [31] L. Vakeva, A. Ranki, S. Hahtola, *Acta Derm Venereol*, 92 (2012) 258-263.
- [32] J.J. Scarisbrick, S. Morris, R. Azurdia, T. Illidge, E. Parry, R. Graham-Brown, R. Cowan, E. Gallop-Evans, R. Wachsmuth, M. Eagle, A.S. Wierzbicki, H. Soran, S. Whittaker, E.M. Wain, *British Journal of Dermatology*, 168 (2013) 192-200.
- [33] W.H. Ang, A. De Luca, C. Chapuis-Bernasconi, L. Juillerat-Jeanneret, M. Lo Bello, P.J. Dyson, *ChemMedChem*, 2 (2007) 1799-1806.
- [34] C.A. Vock, W.H. Ang, C. Scolaro, A.D. Phillips, L. Lagopoulos, L. Juillerat-Jeanneret, G. Sava, R. Scopelliti, P.J. Dyson, *Journal of Medicinal Chemistry*, 50 (2007) 2166-2175.
- [35] A.A. Nazarov, D. Gardini, M. Baquie, L. Juillerat-Jeanneret, T.P. Serkova, E.P. Shevtsova, R. Scopelliti, P.J. Dyson, *Dalton Transactions*, 42 (2013) 2347-2350.
- [36] M. Patra, G. Gasser, *ChemBioChem*, 13 (2012) 1232-1252.
- [37] H. Zhang, R. Zhou, L. Li, J. Chen, L. Chen, C. Li, H. Ding, L. Yu, L. Hu, H. Jiang, X. Shen, *J. Biol. Chem.*, 286 (2011) 1868-1875.
- [38] W.L.F. Armarego, C. Chai, *Purification of Laboratory Chemicals*, 5th ed., Butterworth-Heinemann, Oxford, 2003.
- [39] F. Neese, *Wiley Interdiscip. Rev.: Comput. Mol. Sci.*, 2 (2012) 73-78.
- [40] A.D. Becke, *Phys. Rev. A*, 38 (1988) 3098-3100.
- [41] C. Lee, W. Yang, R.G. Parr, *Phys. Rev. B*, 37 (1988) 785-789.
- [42] S.H. Vosko, L. Wilk, M. Nusair, *Can. J. Phys.*, 58 (1980) 1200-1211.
- [43] Y. Zhao, D.G. Truhlar, *Theor. Chem. Acc.*, 120 (2008) 215-241.
- [44] Y. Zhao, D.G. Truhlar, *J. Chem. Phys.*, 125 (2006) 194101.
- [45] P.J. Hay, W.R. Wadt, *J. Chem. Phys.*, 82 (1985) 299-310.
- [46] P.F. Egea, A. Mitschler, D. Moras, *Mol. Endocrinol.*, 16 (2002) 987-997.
- [47] T.A.D. D.A. Case, T.E. Cheatham, III, C.L. Simmerling, J. Wang, R.E. Duke, R. Luo, R.C. Walker, W. Zhang, K.M. Merz, B. Roberts, B. Wang, S. Hayik, A. Roitberg, G. Seabra, I. Kolossváry, K.F. Wong, F. Paesani, J. Vanicek, J. Liu, X. Wu, S.R. Brozell, T. Steinbrecher, H. Gohlke, Q. Cai, X. Ye, J. Wang, M.-J. Hsieh, G. Cui, D.R. Roe, D.H. Mathews, M.G. Seetin, C. Sagui, V. Babin, T. Luchko, S. Gusarov, A. Kovalenko, and P.A. Kollman AMBER 11 University of California, San Francisco., (2010).
- [48] J. Wang, R.M. Wolf, J.W. Caldwell, P.A. Kollman, D.A. Case, *J. Comput. Chem.*, 25 (2004) 1157-1174.
- [49] A. Jakalian, D.B. Jack, C.I. Bayly, *J. Comput. Chem.*, 23 (2002) 1623-1641.
- [50] J.D. Durrant, J.A. McCammon, *J. Mol. Graphics Modell.*, 31 (2011) 5-9.
- [51] F. Fogolari, A. Brigo, H. Molinari, *Biophys. J.*, 85 159-166.
- [52] W. Humphrey, A. Dalke, K. Schulten, *J. Mol. Graphics*, 14 (1996) 33-38.
- [53] G.M. Morris, R. Huey, W. Lindstrom, M.F. Sanner, R.K. Belew, D.S. Goodsell, A.J. Olson, *J. Comput. Chem.*, 30 (2009) 2785-2791.
- [54] A.K. Rappe, C.J. Casewit, K.S. Colwell, W.A. Goddard, W.M. Skiff, *J. Am. Chem. Soc.*, 114 (1992) 10024-10035.

Highlights:

- Synthesis of the imidazole ligands modified with bexarotene and Ru(arene) compounds
- Docking studies with retinoid X receptor
- Cytotoxic behavior of organometallic compounds and ligands.

ACCEPTED MANUSCRIPT